



10th Time-Dependent Density-Functional Theory:
Prospects and Applications
Benasque Science Center, Spain
2025.4.14-16(15)

TDDFT for extremely nonlinear light propagation

Kazuhiro Yabana

Center for Computational Sciences,
University of Tsukuba



Benasque, Telluride, and in Asia

Dr. Tomohito Otohe (QST, Kyoto) is organizing a School/Workshop in **Nara**.



Photo: Kazuyoshi Miyoshi
撮影:三好 和義

**2nd International Symposium on
Ab-Initio Electron Dynamics Simulation
(AIEDS2)**

School & SALMON Hands On: March 9-10, 2026
Workshop: March 11-13, 2026
Venue: Kinsho Hall, Todai-ji at Nara, Japan



Todaiji-temple: world heritage, largest wooden structure in the world

Combine Maxwell equations and TDDFT

Light propagation solving classical Maxwell's equations

$$\nabla \times \nabla \times \mathbf{A} + \frac{1}{c^2} \frac{\partial^2}{\partial t^2} \mathbf{A} = \frac{4\pi}{c} \mathbf{j}$$

Electron dynamics by TDDFT in real time

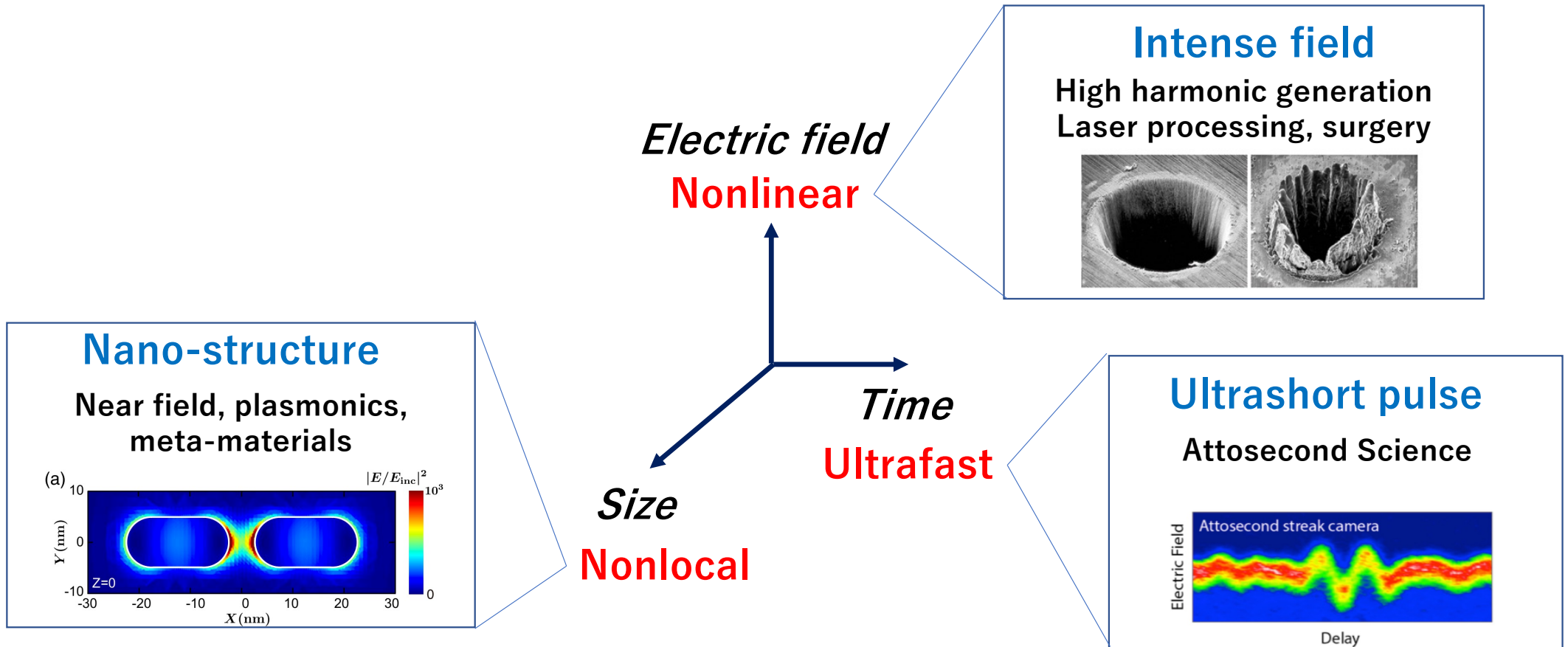
$$i\hbar \frac{\partial}{\partial t} \psi_i = \left\{ \frac{1}{2m} \left(-i\hbar \nabla + \frac{e}{c} \mathbf{A} \right)^2 + V_{ion} + V_H + V_{xc} \right\} \psi_i$$
$$\mathbf{j} = -\frac{e}{2m} \left\{ \psi_i^* \left(-i\hbar \nabla + \frac{e}{c} \mathbf{A} \right) \psi_i + c.c. \right\}$$

Contents

- **About “Extreme Optics”**
- **Maxwell-TDDFT**
- **Some applications**
- **Maxwell-TDDFT at oblique incidence (under progress)**
- **Dephasing and density-matrix unfolding (under progress)**

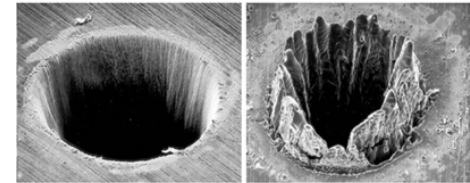
Extreme Optics

Frontiers of optical science using extreme pulsed light



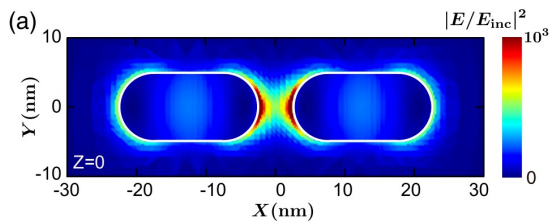
Intense field

High harmonic generation
Laser processing, surgery



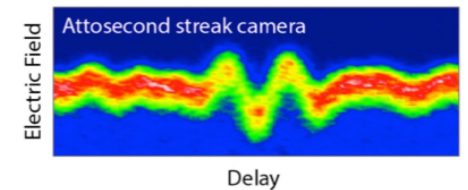
Nano-structure

Near field, plasmonics,
meta-materials



Ultrashort pulse

Attosecond Science



In extreme optics, ordinary approach is not sufficient

Light propagation (Maxwell's) eq.

$$\begin{aligned}\nabla \cdot \mathbf{B} &= 0 \\ \nabla \times \mathbf{E} + \frac{\partial \mathbf{B}}{\partial t} &= \mathbf{0} \\ \nabla \cdot \mathbf{D} &= \rho \\ \nabla \times \mathbf{H} - \frac{\partial \mathbf{D}}{\partial t} &= \mathbf{j}\end{aligned}$$

e.g, FDTD (Finite-difference time-domain method)

Electromagnetism (EM)

First-principles quantum mechanics calculations of optical constants

Constitutive relation

$$\begin{aligned}\mathbf{D}(\mathbf{r}, t) &= \int_{-\infty}^t dt' \epsilon(t-t') \mathbf{E}(\mathbf{r}, t') \\ \mathbf{D}(\mathbf{r}, \omega) &= \epsilon(\omega) \mathbf{E}(\mathbf{r}, \omega)\end{aligned}$$

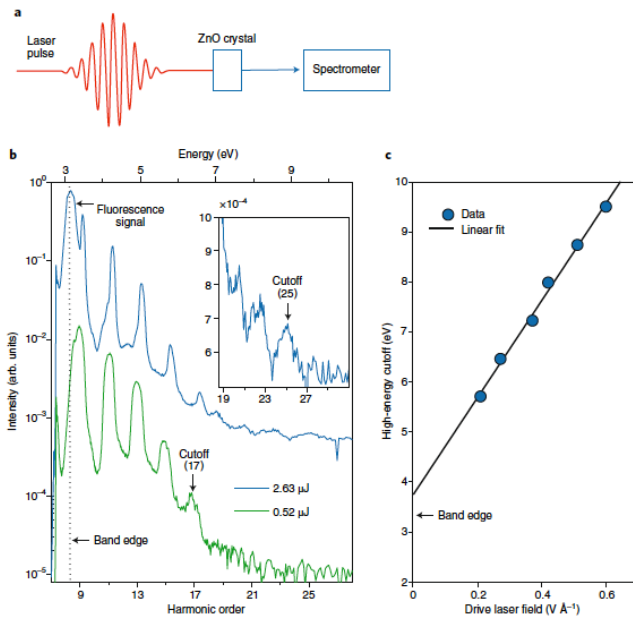
$$\epsilon_r = 1 + \frac{2Ne^2}{\epsilon_0 \hbar} \sum_j \frac{\omega_{j0} |\langle 0 | x | j \rangle|^2}{\omega_{j0}^2 - (\omega + i\gamma)^2}$$

e.g, GW-BSE, TDDFT

Quantum Mechanics (QM)

Nonlinearity: strong laser pulse on materials

High harmonic generation from solids



S. Ghimire et al, Nat. Phys. 7, 138 (2011)
 S. Ghimire, D.A. Reis, Nature Physics 15, 10 (2019)

$$P(\mathbf{r}, t) = \int dt' \chi^{(1)}(t - t') E(\mathbf{r}, t')$$



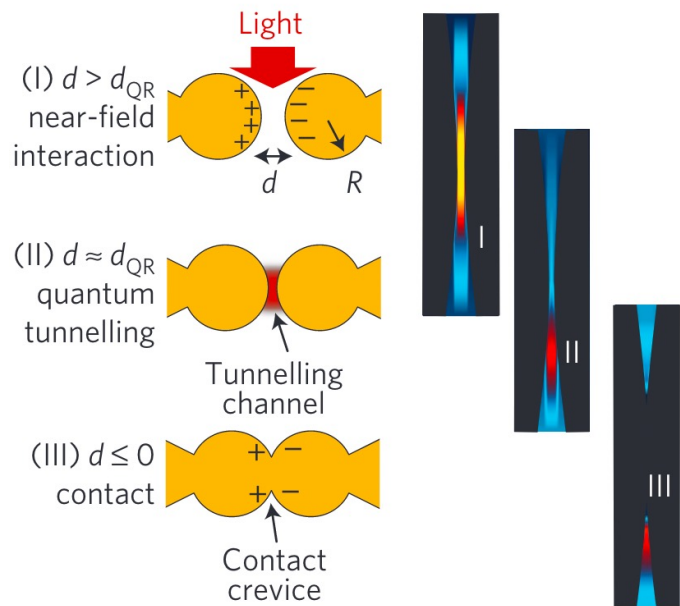
$$P(\mathbf{r}, t) = \int dt' \chi^{(1)}(t - t') E(\mathbf{r}, t') + \int dt' dt'' \chi^{(2)}(t - t', t - t'') E(\mathbf{r}, t') E(\mathbf{r}, t'') + \int dt' dt'' dt''' \chi^{(3)}(t - t', t - t'', t - t''') E(\mathbf{r}, t') E(\mathbf{r}, t'') E(\mathbf{r}, t''') + \dots$$

Spatially local, but highly nonlinear

Explicit construction of nonlinear susceptibilities is difficult and useless.

Nonlocality: optical response in nano-material

Quantum Tunneling in Plasmonics



M.S. Tame et.al, Nature Phys. 9, 329 (2013)

$$P(\mathbf{r}, t) = \int dt' \chi^{(1)}(t - t') E(\mathbf{r}, t')$$



$$P(\mathbf{r}, t) = \int dt' \int d\mathbf{r}' \chi^{(1)}(\mathbf{r}, \mathbf{r}', t - t') E(\mathbf{r}', t')$$

Linear, but spatially nonlocal

Explicit construction of nonlocal susceptibility is difficult and useless.

Contents

- About “Extreme Optics”
- **Maxwell-TDDFT**
- Some applications
- Maxwell-TDDFT at oblique incidence (under progress)
- Dephasing and density-matrix unfolding (under progress)

We combine EM and QM

Light propagation solving classical Maxwell's equations

$$\nabla \times \nabla \times \mathbf{A} + \frac{1}{c^2} \frac{\partial^2}{\partial t^2} \mathbf{A} = \frac{4\pi}{c} \mathbf{j}$$

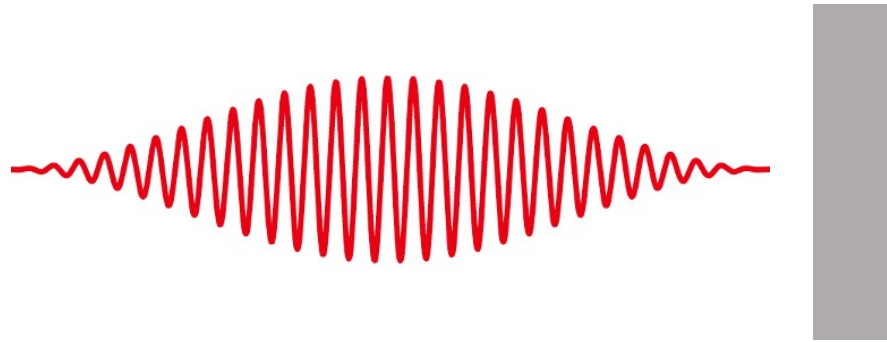
Electron dynamics by TDDFT in real time

$$i\hbar \frac{\partial}{\partial t} \psi_i = \left\{ \frac{1}{2m} \left(-i\hbar \nabla + \frac{e}{c} \mathbf{A} \right)^2 + V_{ion} + V_H + V_{xc} \right\} \psi_i$$
$$\mathbf{j} = -\frac{e}{2m} \left\{ \psi_i^* \left(-i\hbar \nabla + \frac{e}{c} \mathbf{A} \right) \psi_i + c.c. \right\}$$

We develop two connection methods, without/with coarse-graining.

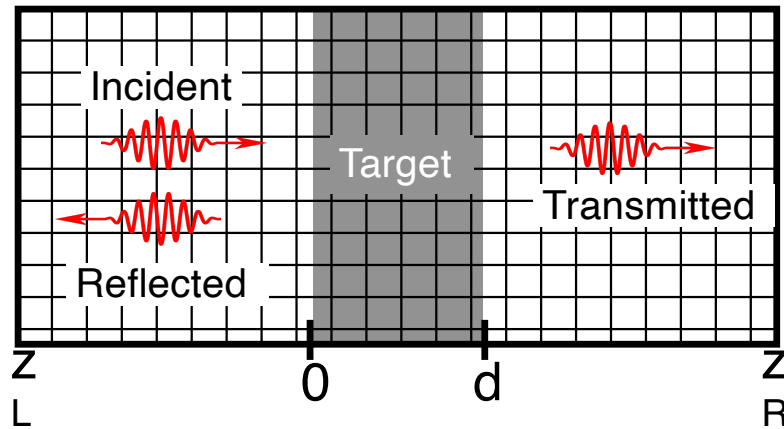
Microscopic (single-grid) vs Macroscopic (multi-grid)

Pulsed light on thin films at normal incidence



Microscopic (Single-scale) vs. Macroscopic (Multi-scale)

Microscopic Maxwell+TDDFT



$$i \frac{\partial}{\partial t} u_{nk} = \hat{H}_{\mathbf{k} + \frac{1}{c} \mathbf{A}(\mathbf{r}, t)} u_{nk}$$

$$\left(\frac{1}{c^2} \frac{\partial^2}{\partial t^2} - \nabla^2 \right) \mathbf{A}(\mathbf{r}, t) + \frac{1}{c} \nabla \dot{\phi}(\mathbf{r}, t) = -\frac{4\pi}{c} \mathbf{j}_e(\mathbf{r}, t)$$

$$\nabla^2 \phi(\mathbf{r}, t) = 4\pi n_e(\mathbf{r}, t)$$

Single-scale approach using a common spatial grid

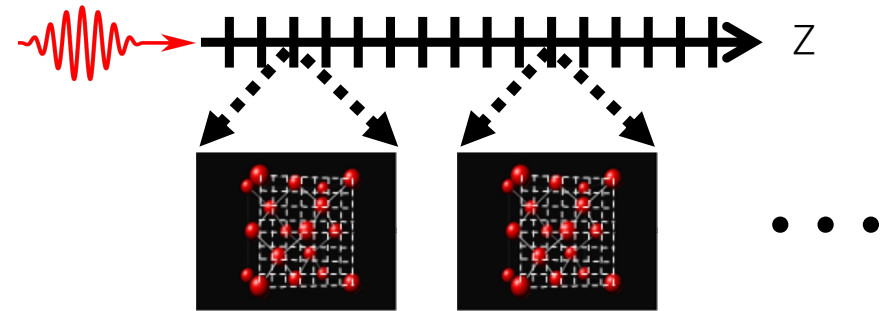
nonlocal + nonlinear

S. Yamada *et al.*, PRB **98**, 245147 (2018).

Macroscopic Maxwell+TDDFT

$$\left(\frac{1}{c^2} \frac{\partial^2}{\partial t^2} - \frac{\partial^2}{\partial Z^2} \right) \mathbf{A}_Z(t) = \frac{4\pi}{c} \mathbf{J}_Z(t)$$

grid spacing ~ 10 nm



nm-scale grid #1

nm-scale grid #2

$$i \frac{\partial}{\partial t} u_{nk,Z} = \hat{H}_{\mathbf{k} + \frac{1}{c} \mathbf{A}_Z(t)} u_{nk,Z}$$

$$i \frac{\partial}{\partial t} u_{nk,Z} = \hat{H}_{\mathbf{k} + \frac{1}{c} \mathbf{A}_Z(t)} u_{nk,Z}$$

Multiscale approach using different spatial grid

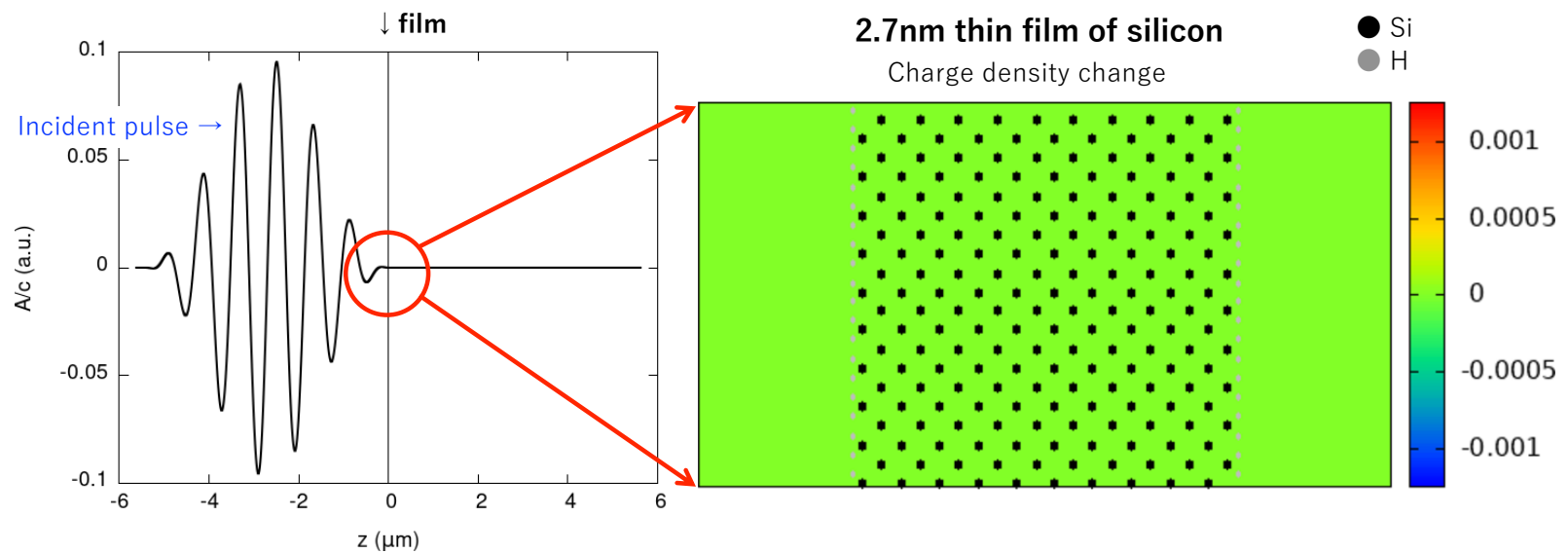
nonlinear only

K. Yabana *et al.*, PRB **85**, 045134 (2012).

Microscopic (single-scale) Maxwell-TDDFT: pulsed light on Si nano-film



Shunsuke Yamada
Kansai Photon Sci. Inst

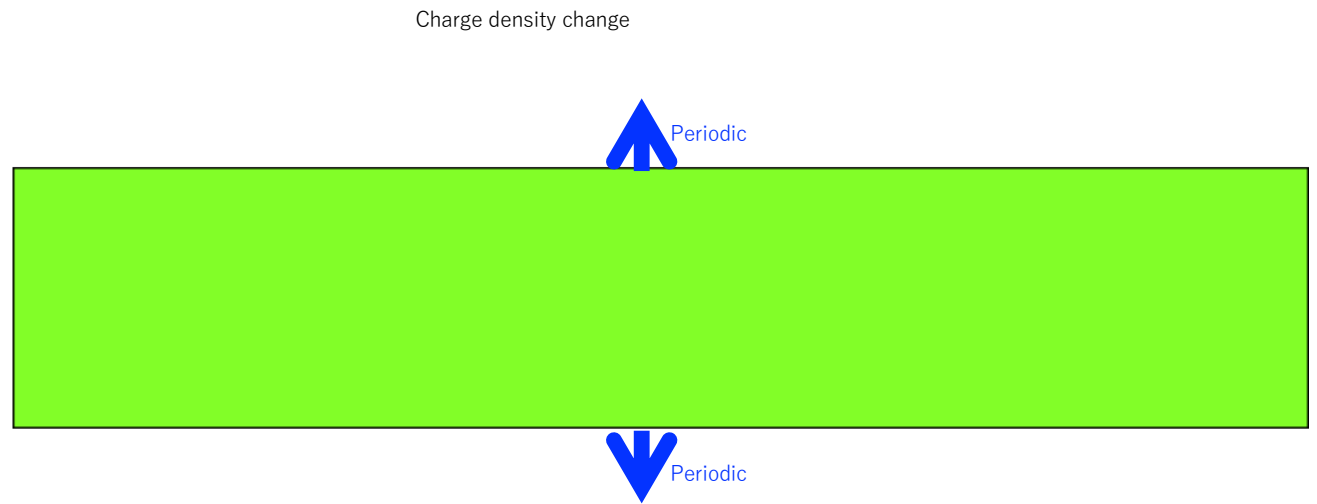
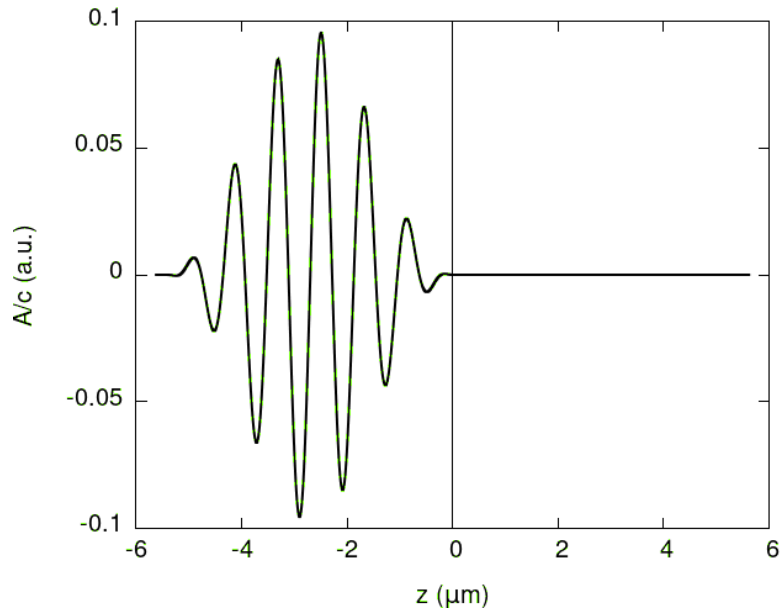


Light wavelength 800nm

Nonlocal + Nonlinear

Thicker film (27.2nm)

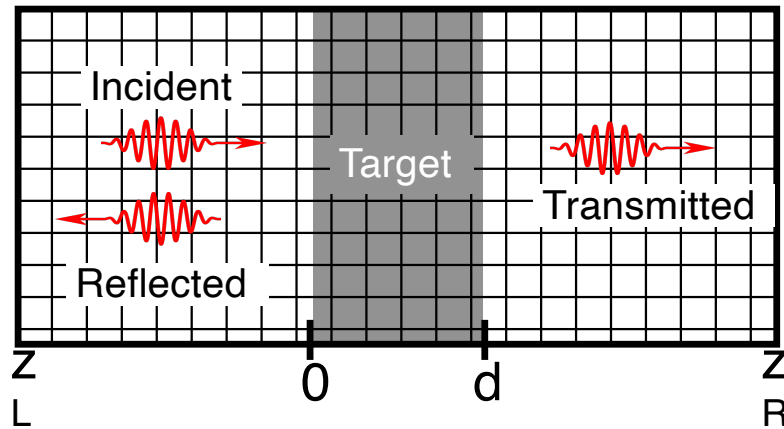
Light pulse: $\hbar\omega = 1.5\text{eV}$, $I = 10^{12}\text{W/cm}^2$, $T = 18\text{fs}$



**Max. possible thickness $\sim 50\text{nm}$
limited by computational capability**

Microscopic (Single-scale) vs. Macroscopic (Multi-scale)

Microscopic Maxwell+TDDFT



$$i \frac{\partial}{\partial t} u_{n\mathbf{k}} = \hat{H}_{\mathbf{k} + \frac{1}{c} \mathbf{A}(\mathbf{r}, t)} u_{n\mathbf{k}}$$

$$\left(\frac{1}{c^2} \frac{\partial^2}{\partial t^2} - \nabla^2 \right) \mathbf{A}(\mathbf{r}, t) + \frac{1}{c} \nabla \dot{\phi}(\mathbf{r}, t) = -\frac{4\pi}{c} \mathbf{j}_e(\mathbf{r}, t)$$

$$\nabla^2 \phi(\mathbf{r}, t) = 4\pi n_e(\mathbf{r}, t)$$

Single-scale approach using a common spatial grid

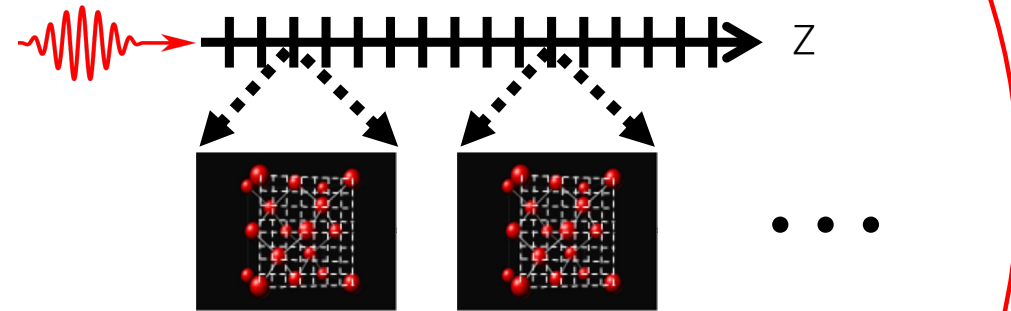
nonlocal + nonlinear

S. Yamada *et al.*, PRB **98**, 245147 (2018).

Macroscopic Maxwell+TDDFT

$$\left(\frac{1}{c^2} \frac{\partial^2}{\partial t^2} - \frac{\partial^2}{\partial Z^2} \right) \mathbf{A}_Z(t) = \frac{4\pi}{c} \mathbf{J}_Z(t)$$

grid spacing ~ 10 nm



nm-scale grid #1

nm-scale grid #2

$$i \frac{\partial}{\partial t} u_{n\mathbf{k}, Z} = \hat{H}_{\mathbf{k} + \frac{1}{c} \mathbf{A}_Z(t)} u_{n\mathbf{k}, Z}$$

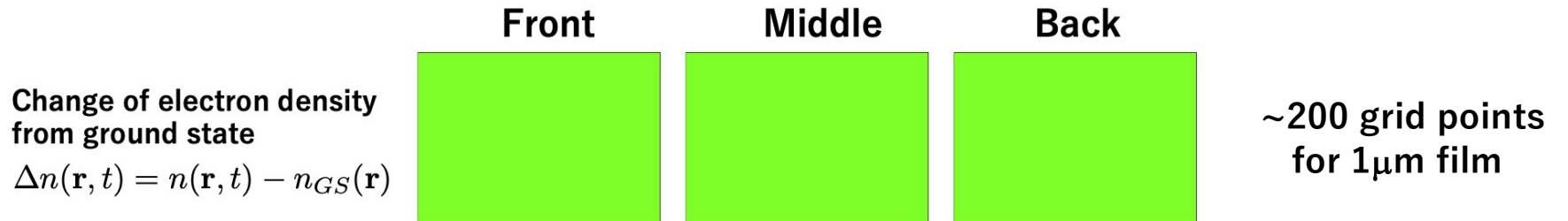
$$i \frac{\partial}{\partial t} u_{n\mathbf{k}, Z} = \hat{H}_{\mathbf{k} + \frac{1}{c} \mathbf{A}_Z(t)} u_{n\mathbf{k}, Z}$$

Multiscale approach using different spatial grid

nonlinear only

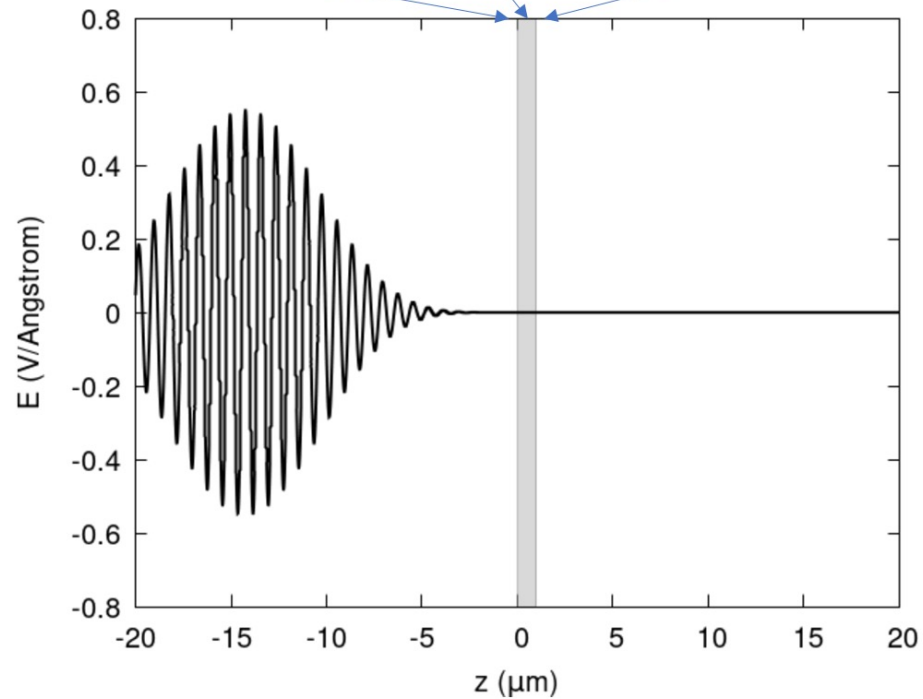
K. Yabana *et al.*, PRB **85**, 045134 (2012).

Macroscopic (multi-scale) Maxwell-TDDFT: pulsed light on 1 μ m Si film



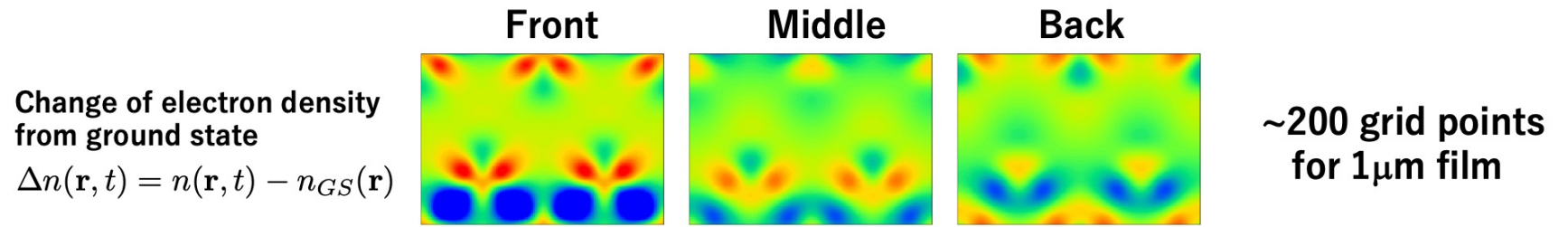
Thin film
Silicon, 1 μ m thick

Laser pulse
800nm (1.55eV=below gap)
 $4 \times 10^{12} \text{W/cm}^2$



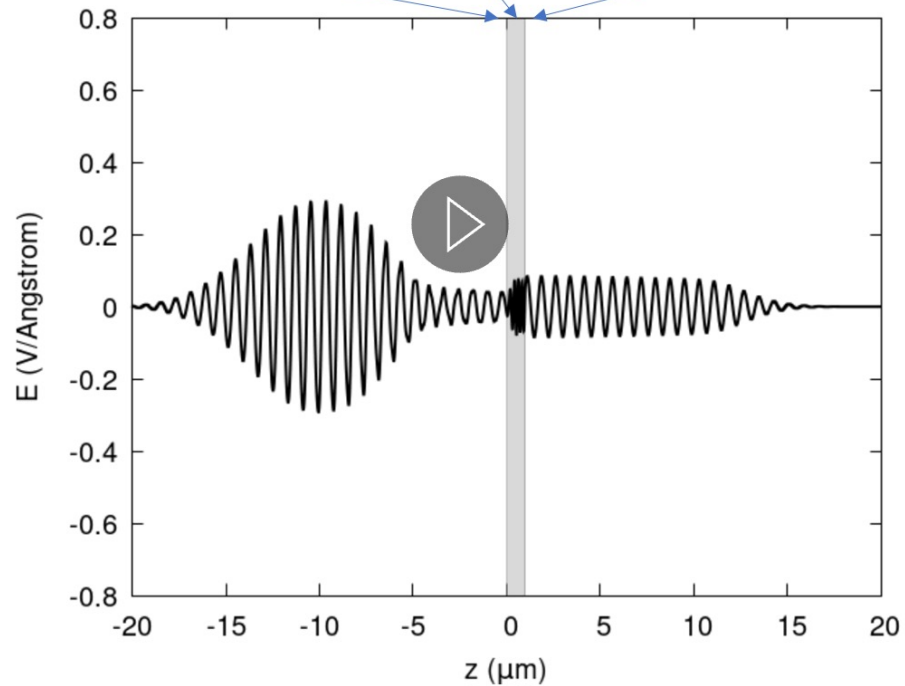
Nonlinear only

Macroscopic (multi-scale) Maxwell-TDDFT: pulsed light on 1 μ m Si film



Thin film
Silicon, 1 μ m thick

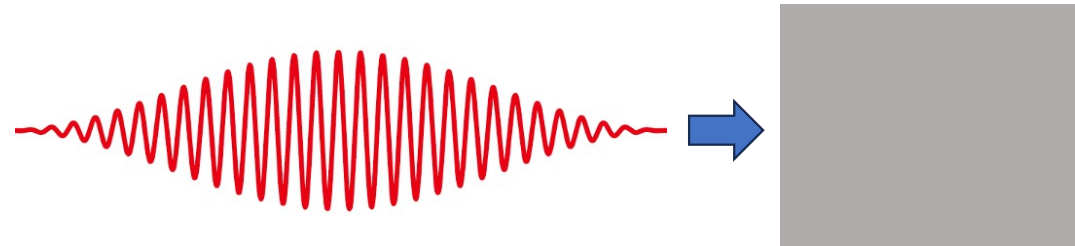
Laser pulse
800nm (1.55eV=below gap)
 $4 \times 10^{12} \text{W/cm}^2$



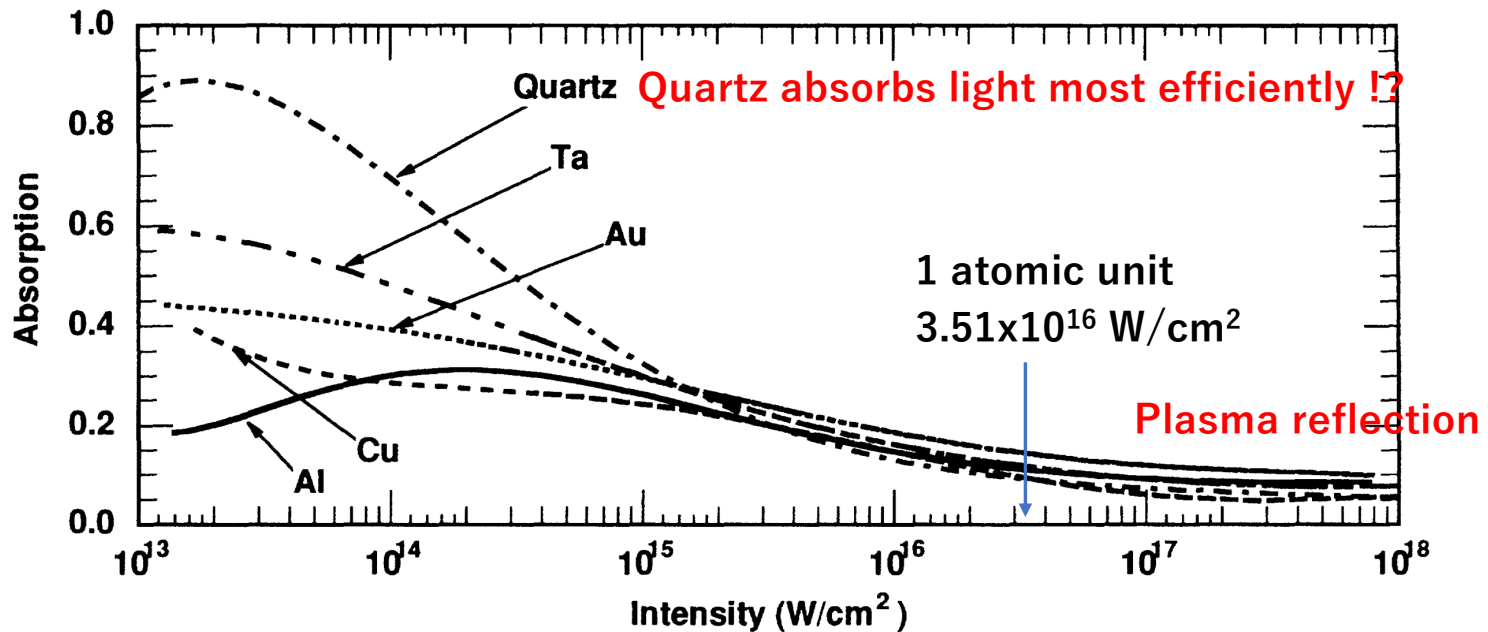
Contents

- About “Extreme Optics”
- Maxwell-TDDFT
- **Some applications**
- Maxwell-TDDFT at oblique incidence (under progress)
- Dephasing and density-matrix unfolding (under progress)

High intensity laser pulse on various materials : Systematics



Absorption
= 1 - Reflection



Experiment at LLNL, using 120fs pulse

D.F.Price et al., *Phys.Rev.Lett.* 75,252 (1995)



Atsushi Yamada
Defence Academy

High intensity laser pulse on various materials : Systematics

Multiscale Maxwell-TDDFT calculation

A. Yamada, K. Yabana, Phys. Rev. B109, 245130 (2024)

Experiment at LLNL, using 120fs pulse

D.F.Price et al., *Phys.Rev.Lett.* **75**,252 (1995)

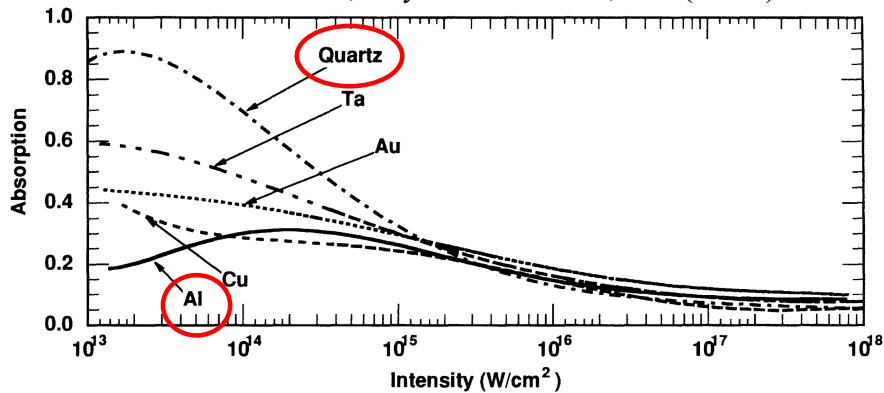
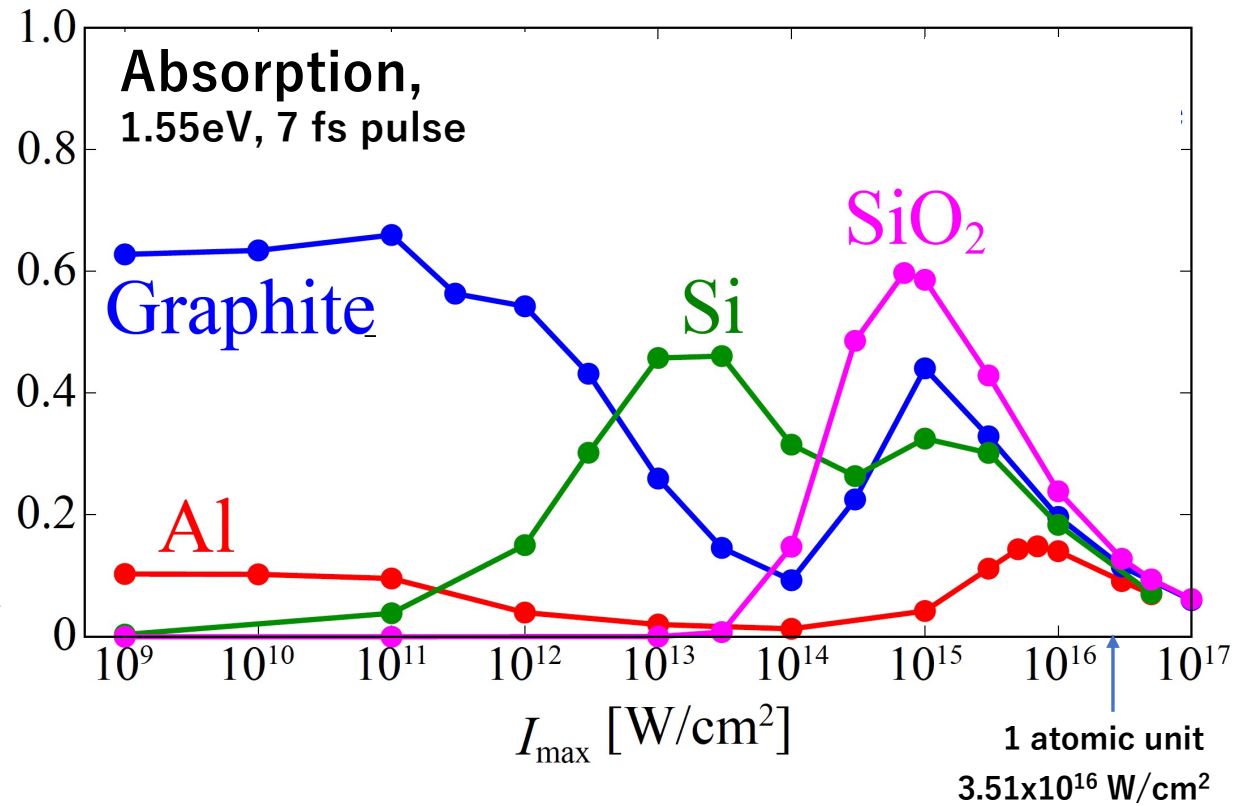
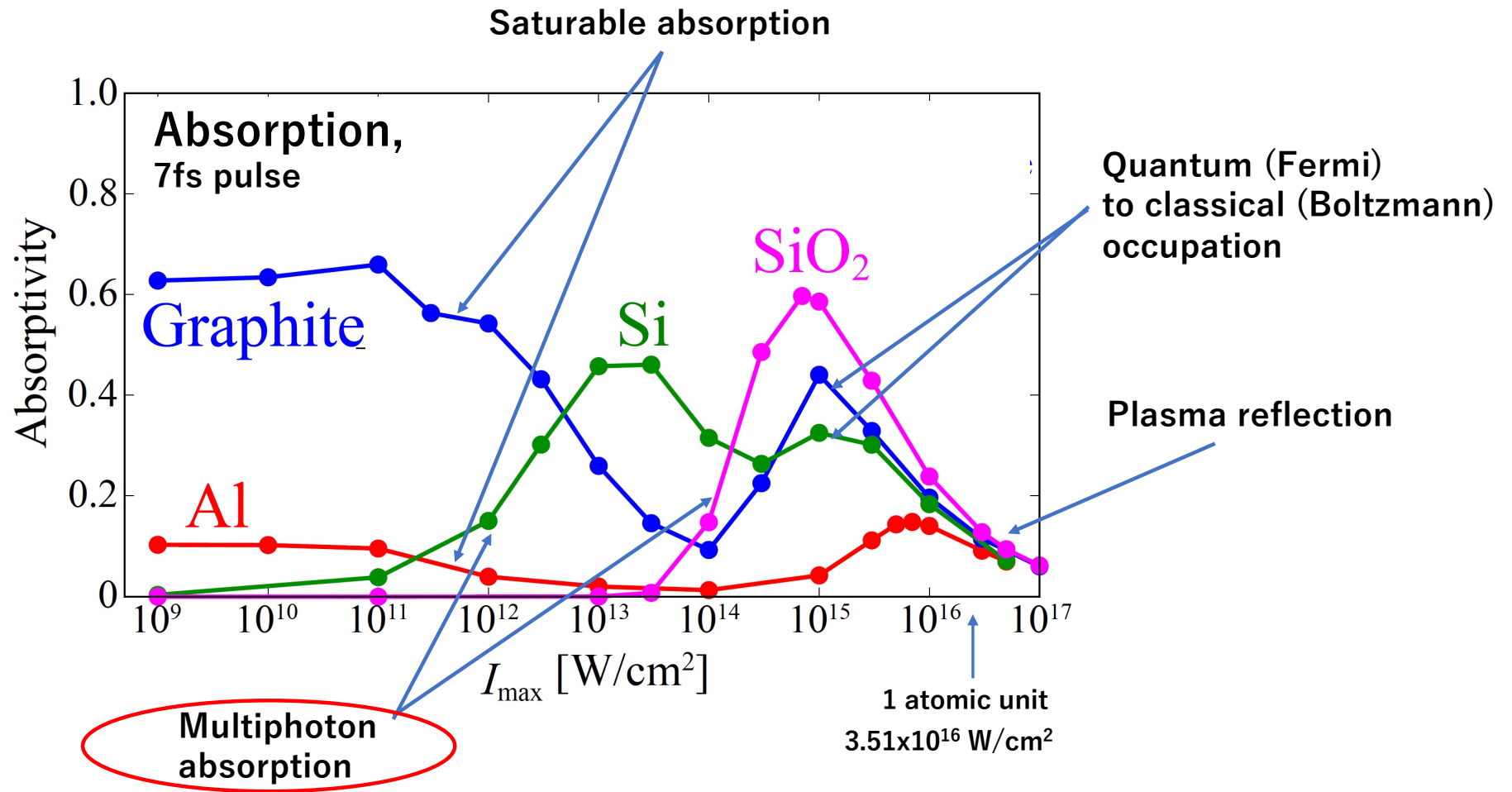


FIG. 1. Absorption fraction vs peak laser intensity for aluminum, copper, gold, tantalum, and quartz targets. In Figs. 1, 3, 4, and 5 laser intensity is the temporal and spatial peak value of the laser intensity.

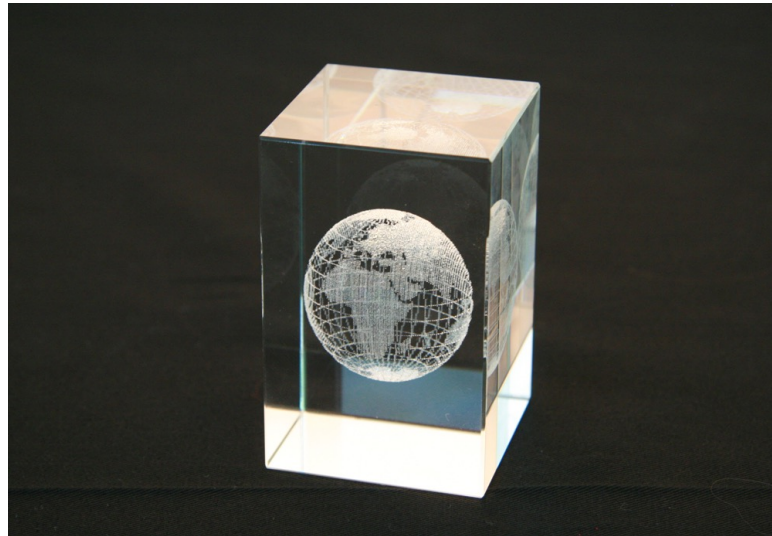


Nonlinear optical response: Mechanisms

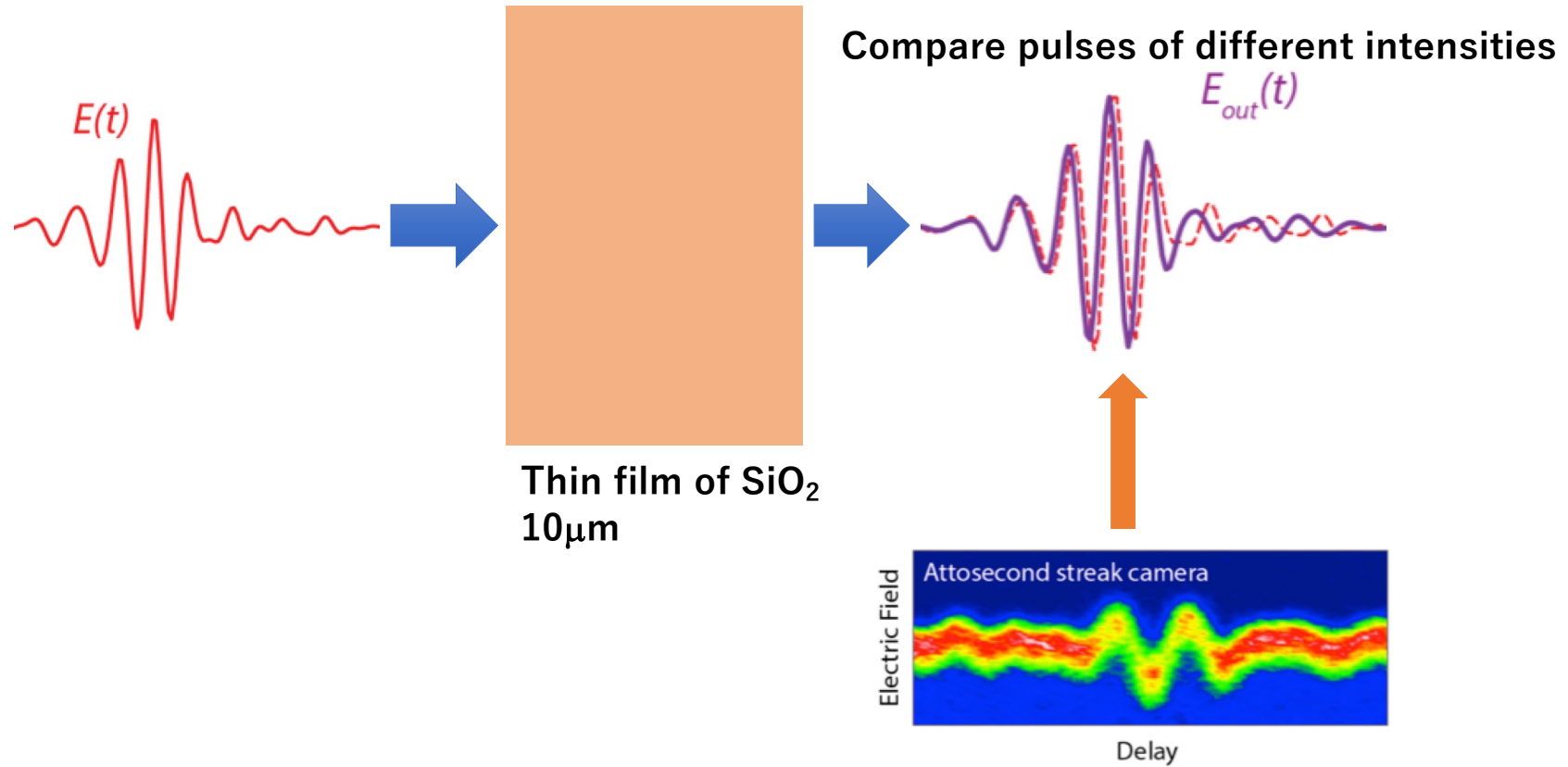


At which intensity of light, glass starts to absorb light?

Laser processing of dielectrics



Laser pulse propagation through SiO₂ 10μm thin film



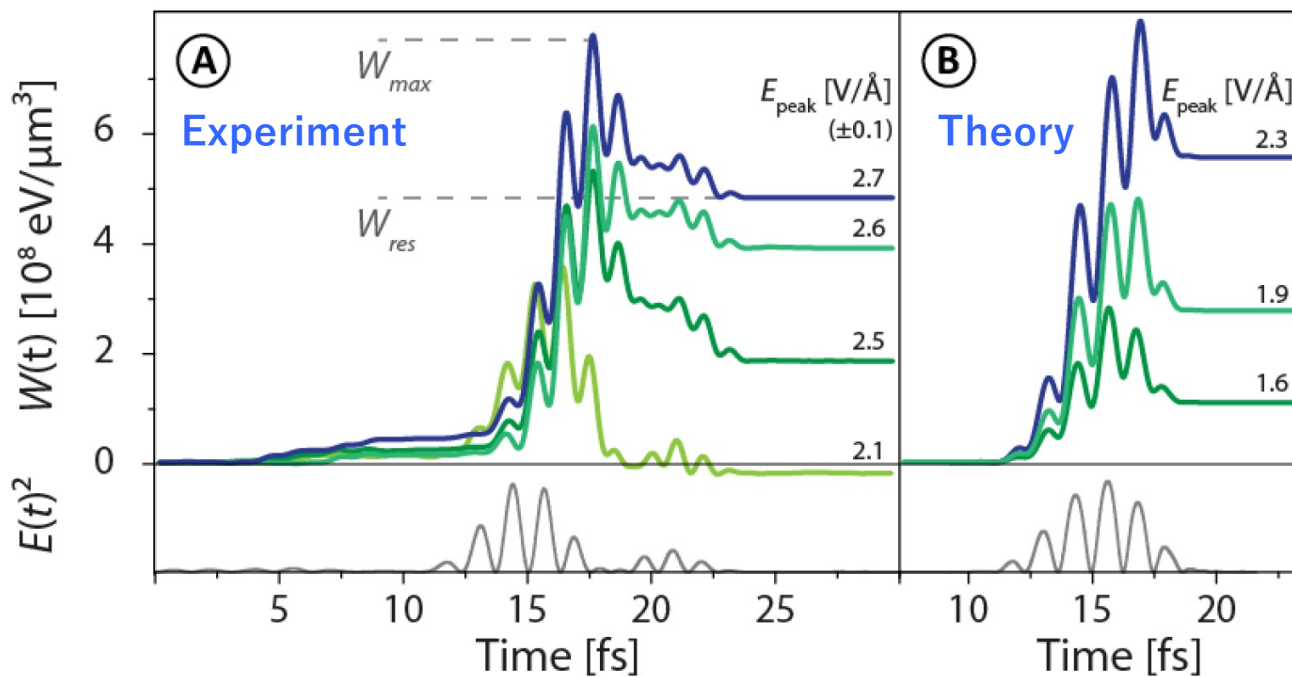
EXP: Attosecond streaking measurements
by Max Planck Inst. Quantum Optics



Energy deposition from laser pulse to SiO₂ at mid point (5μm)

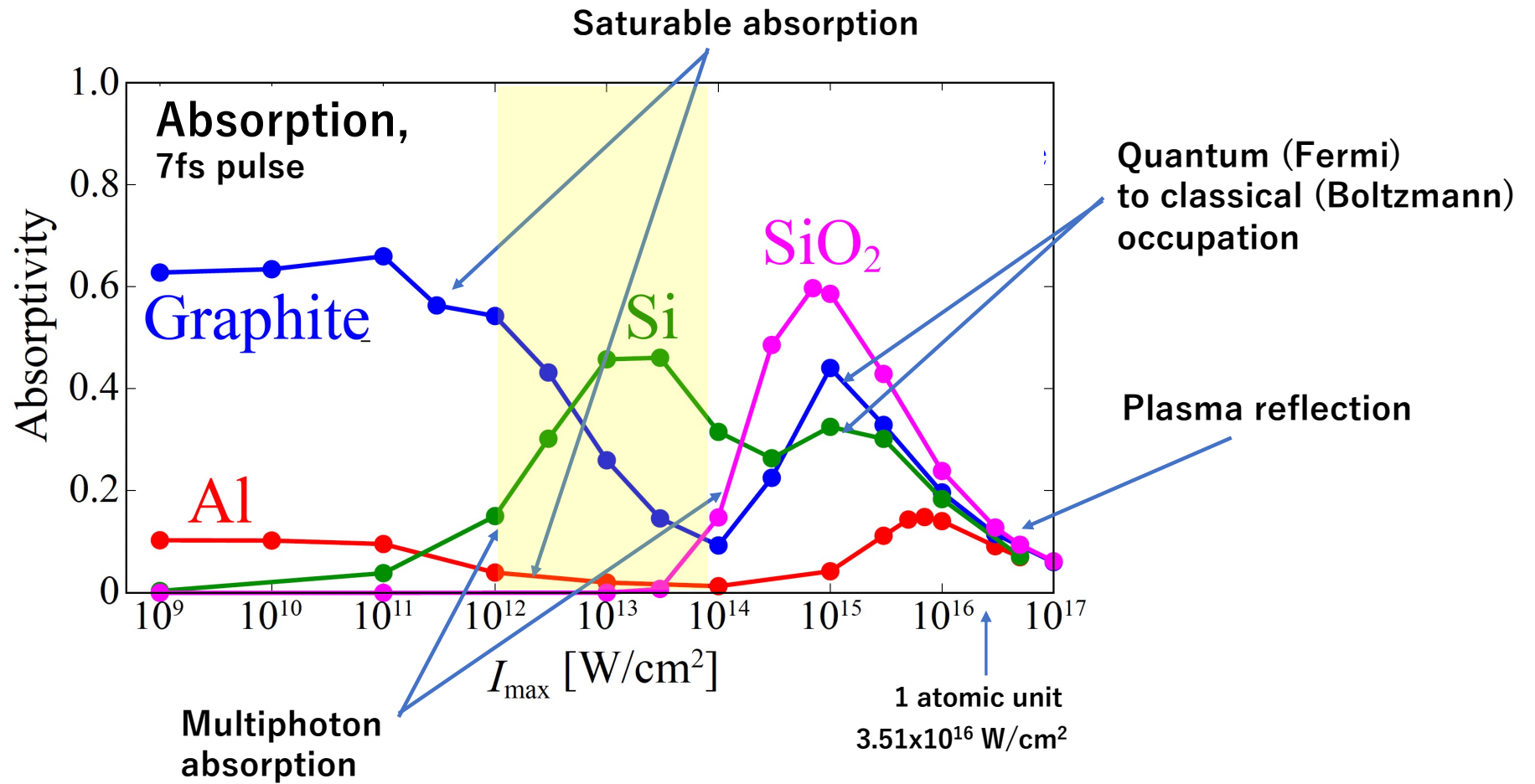
Comparison between theory and experiment

Shunsuke Sato
U. Tsukuba → Tohoku U.



A. Sommer et.al, Nature 534, 86 (2016).
(exp: Max Planck Institute for Quantum Optics)

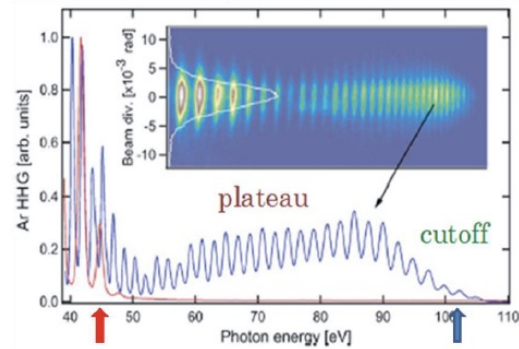
Nonlinear optical response: Mechanisms



High harmonic generation (HHG)

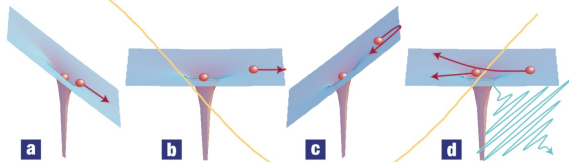
High harmonic generation from atoms

Soft X-ray from visible light



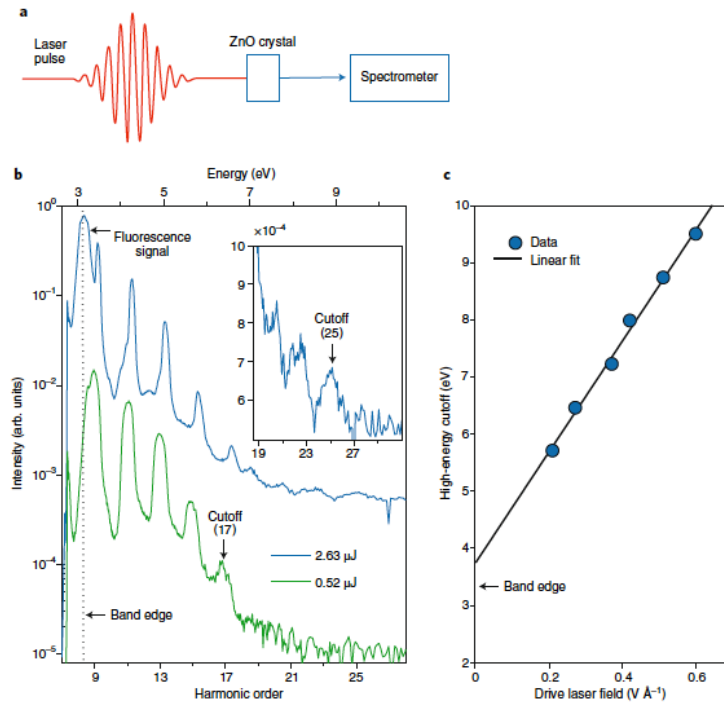
3 step model (electron rescattering)

P.B. Corkum, Phys. Rev. Lett. 71, 1994 (1993)



P.B. Corkum, F. Krausz, Nature Phys. 3, 380 (2007)

High harmonic generation from solids



S. Ghimire et al, Nat. Phys. 7, 138 (2011)

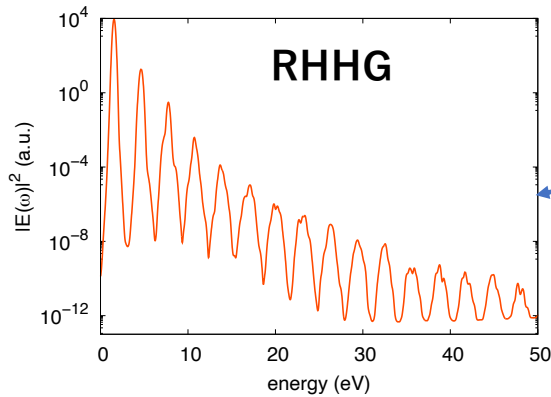
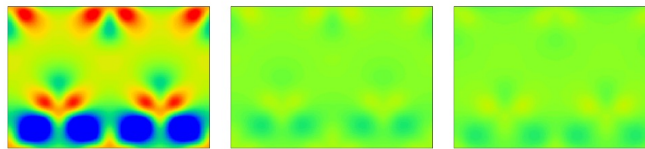
S. Ghimire, D.A. Reis, Nature Physics 15, 10 (2019)

High harmonic components in transmission/reflection waves

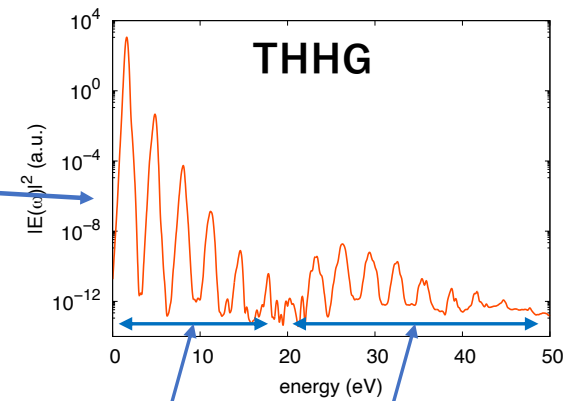
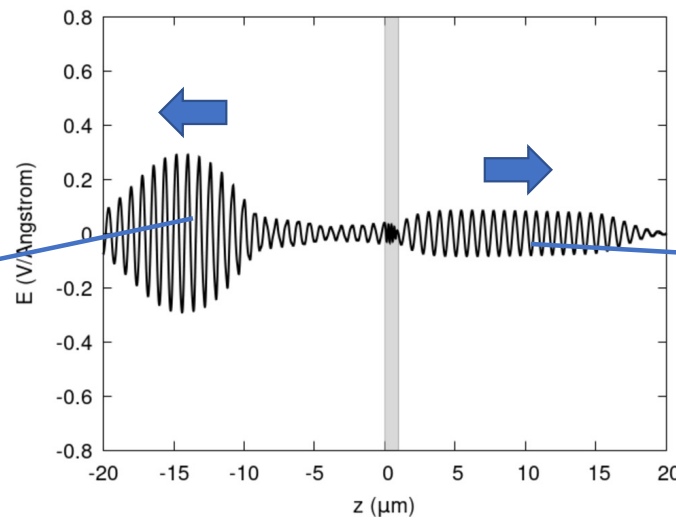
S. Yamada et.al, Phys. Rev. B107, 035132 (2023)

Thin film
Silicon, 1 μm thick

Laser pulse
800nm (1.55eV=below gap)
 $4 \times 10^{12} \text{W}/\text{cm}^2$



Generated at front surface



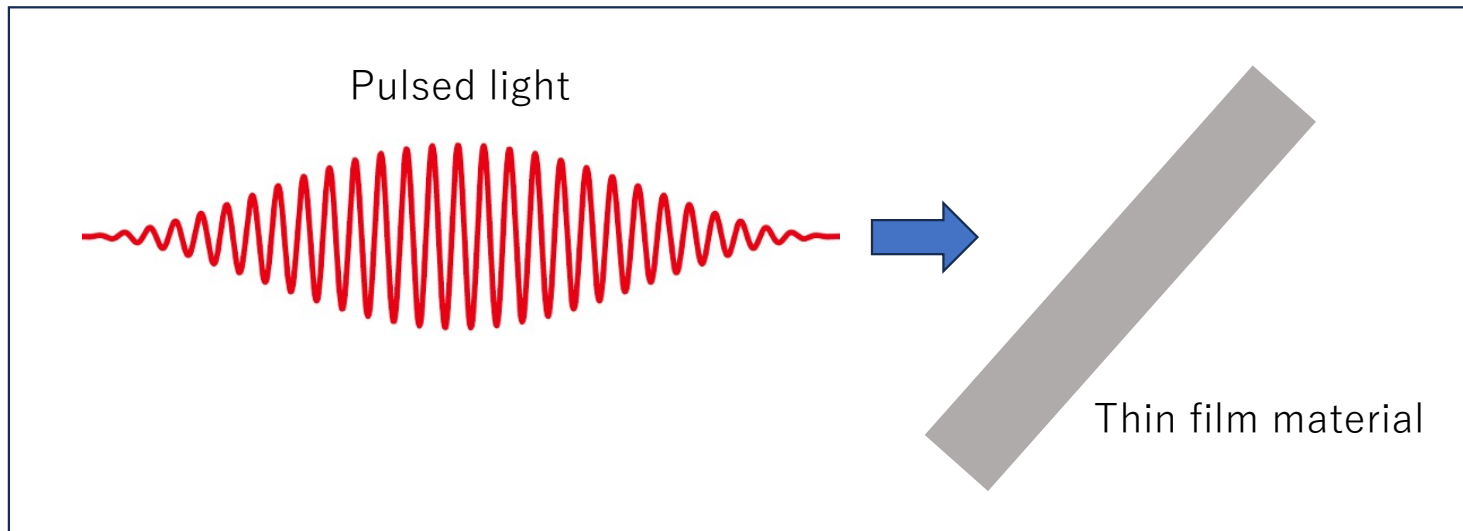
Back surface

Front surface

Contents

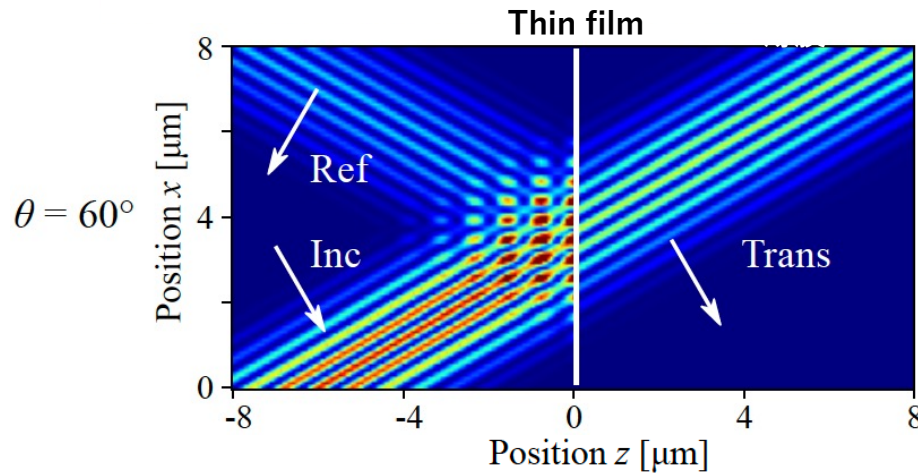
- About “Extreme Optics”
- Maxwell-TDDFT
- Some applications
- **Maxwell-TDDFT at oblique incidence (under progress)**
- Dephasing and density-matrix unfolding (under progress)

An irradiation of a thin material by a pulsed light at oblique incidence



Multiscale Maxwell-TDDFT calculation at oblique incidence

M. Uemoto, K. Yabana, Opt. Exp. 30, 23664 (2022), K. Yabana et.al, in preparation



Translational symmetry
involving time and space

$$\mathbf{A}(\mathbf{R}, t) = \mathbf{a} \left(Z, t - \frac{X \sin \theta}{c} \right)$$

$$\mathbf{J}(\mathbf{R}, t) = \mathbf{j} \left(Z, t - \frac{X \sin \theta}{c} \right)$$

functions of z and t only

$$\nabla \times \mathbf{B} = \frac{4\pi}{c} \mathbf{J} + \frac{1}{c} \frac{\partial}{\partial t} \mathbf{E},$$

$$\nabla \times \mathbf{E} + \frac{1}{c} \frac{\partial}{\partial t} \mathbf{B} = 0,$$



s-polarization

$$\frac{\cos^2 \theta}{c} \frac{\partial}{\partial t} e_y(z, t) = \frac{\partial}{\partial z} b_x(z, t) - \frac{4\pi}{c} j_y(z, t)$$

$$\frac{1}{c} \frac{\partial}{\partial t} b_x(z, t) = \frac{\partial}{\partial z} e_y(z, t)$$

p-polarization

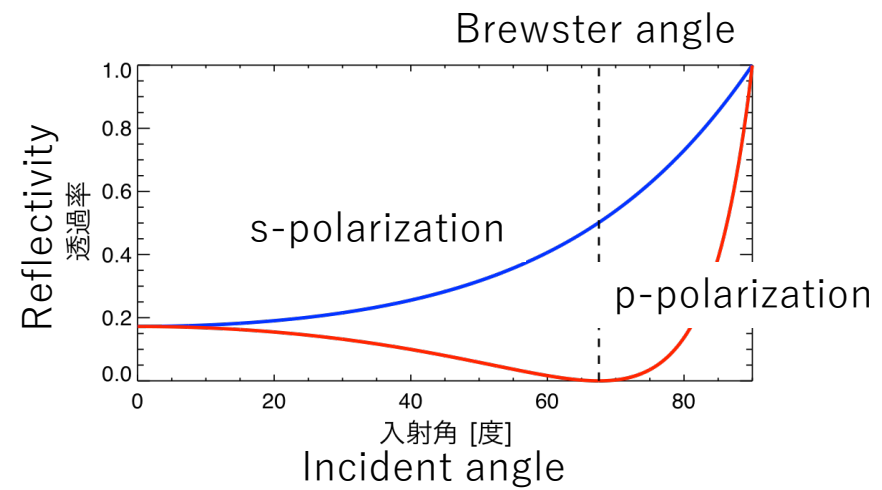
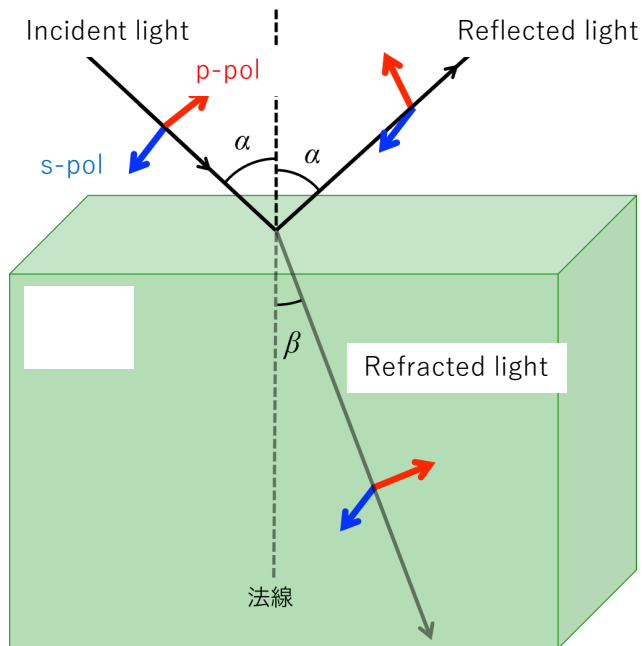
$$\frac{1}{c} \frac{\partial}{\partial t} e_x(z, t) = -\frac{\partial}{\partial z} b_y(z, t) - \frac{4\pi}{c} j_x(z, t)$$

$$\frac{\cos^2 \theta}{c} \frac{\partial}{\partial t} b_y(z, t) = -\frac{\partial}{\partial z} e_x(z, t) + \frac{4\pi}{c} \sin \theta j_z(z, t)$$

Oblique incidence can be calculated with the same computational cost as normal incidence.

Oblique-incident light propagation: linear optics

s- and p-polarizations

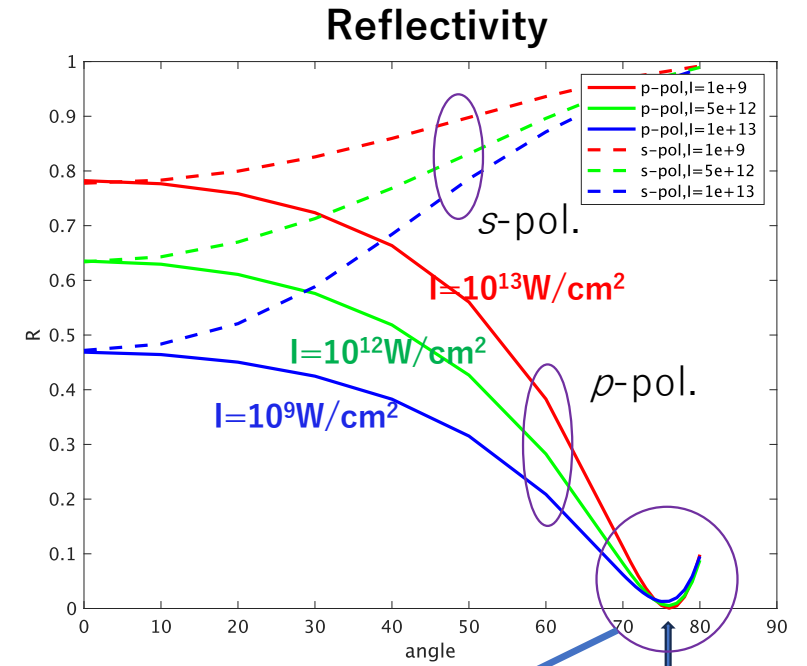
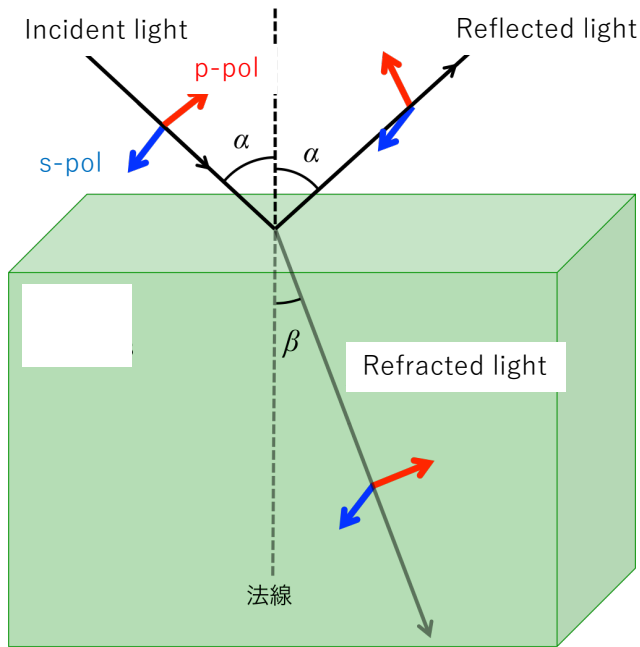


For p-polarization, zero-reflection (Brewster) angle appears.

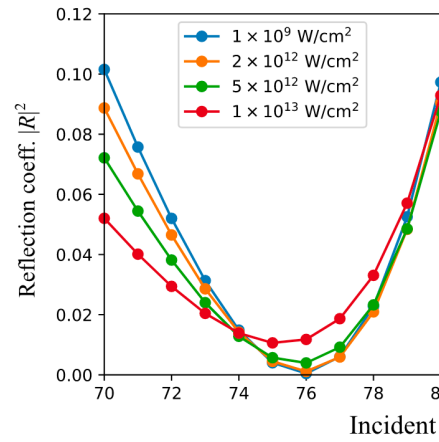
Reflectivity for strong field : Si thin film (50nm)

Brewster's angle appears robustly against intensity

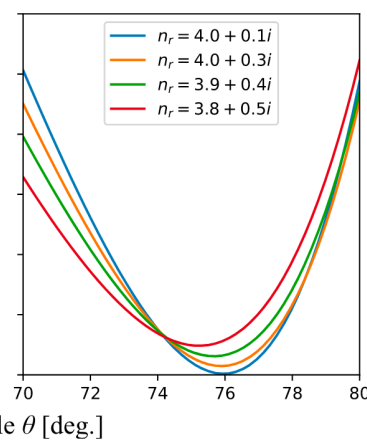
s- and p-polarizations



(a) Oblique Maxwell+TDDFT

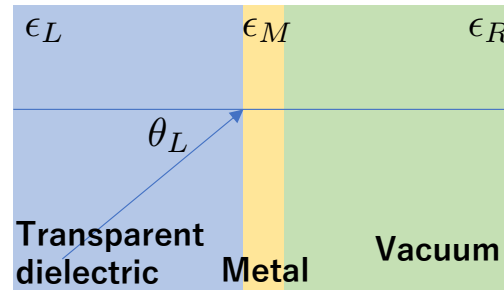


(b) Analytical model



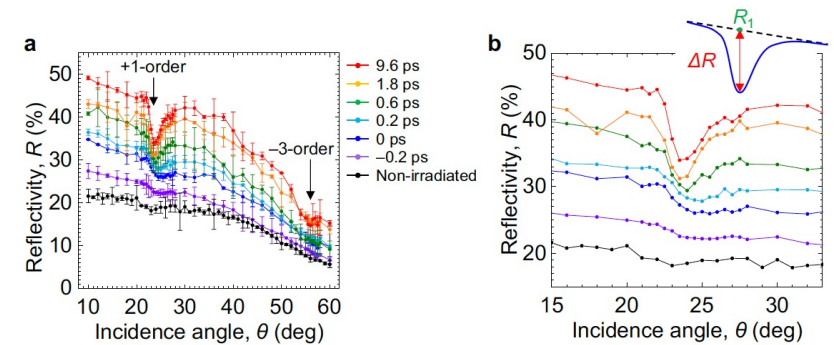
Nonlinearity described by the change of index of refraction

Nonlinearity in Surface Plasmon Polariton?



- Nonlinearity in metals?
- Even dielectrics can produce SPP by metallization?

Indication of SPP in Si
M. Tateda, Y. Iida, G. Miyaji, Sci. Rep. 13, 18414 (2023)



Surface Plasmon Polariton

Linear electromagnetism

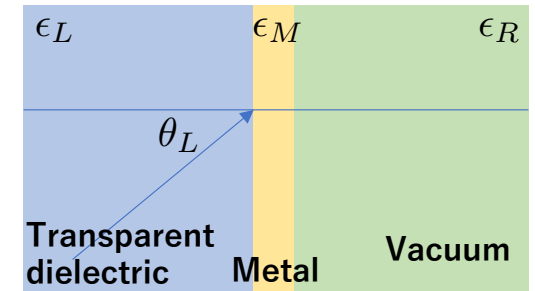
$$R = \left| \frac{A^r}{A^i} \right|^2$$

$$\frac{A^r}{A^i} = -\frac{r_{12} - r_{23}e^{2ik_M d}}{1 - r_{12}r_{23}e^{2ik_M d}}$$

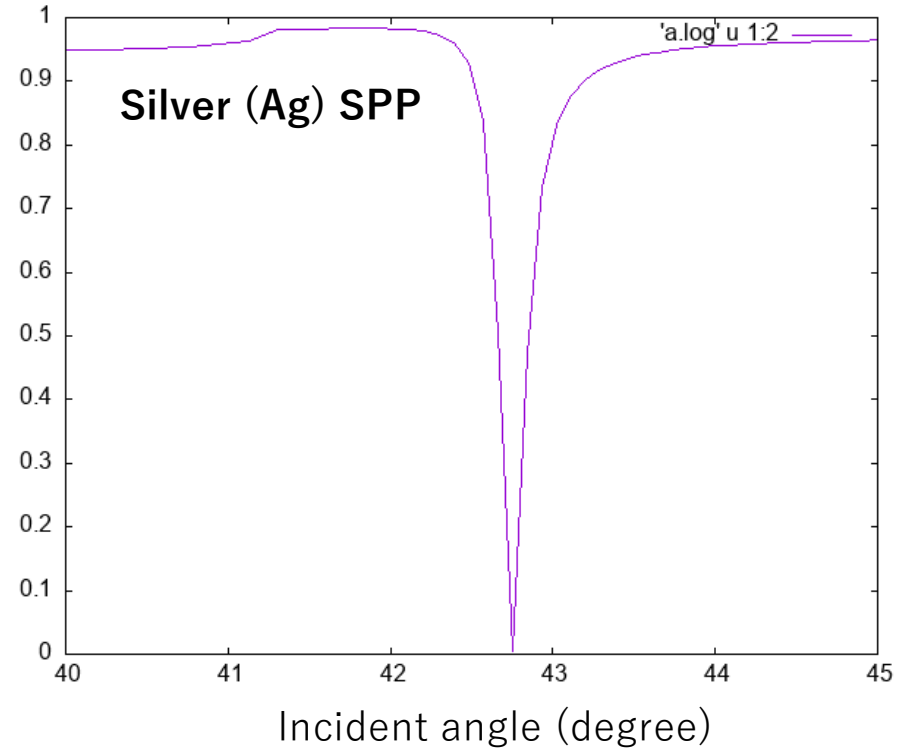
$$r_{12} = \frac{f_{L,-}}{f_{L,+}}, \quad r_{23} = \frac{f_{R,-}}{f_{R,+}} \quad k_M = \frac{\omega}{c} \sqrt{\epsilon_M - n_L^2 \sin^2 \theta_L}$$

$$f_{(R,L),\pm} = n_{(R,L)} \left\{ \frac{\sqrt{\epsilon_{(R,L)} - \epsilon_L \sin^2 \theta_L}}{\epsilon_{(R,L)}} \pm \frac{\sqrt{\epsilon_M - \epsilon_L \sin^2 \theta_L}}{\epsilon_M} \right\}$$

$$\sqrt{\epsilon_R - \epsilon_L \sin^2 \theta_L} \rightarrow i\sqrt{\epsilon_L \sin^2 \theta_L - \epsilon_R}$$



$$\epsilon_L = 2.3, \quad \epsilon_R = 1.0, \quad \epsilon_M = -18.23 + 0.482i, \quad d = 1000 \text{ au} = 52.9 \text{ \AA}.$$

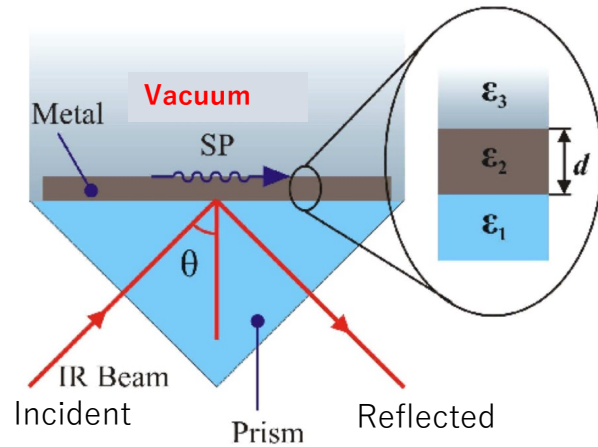


Nonlinear Surface Plasmon Polariton : Aluminum thin film (10nm)

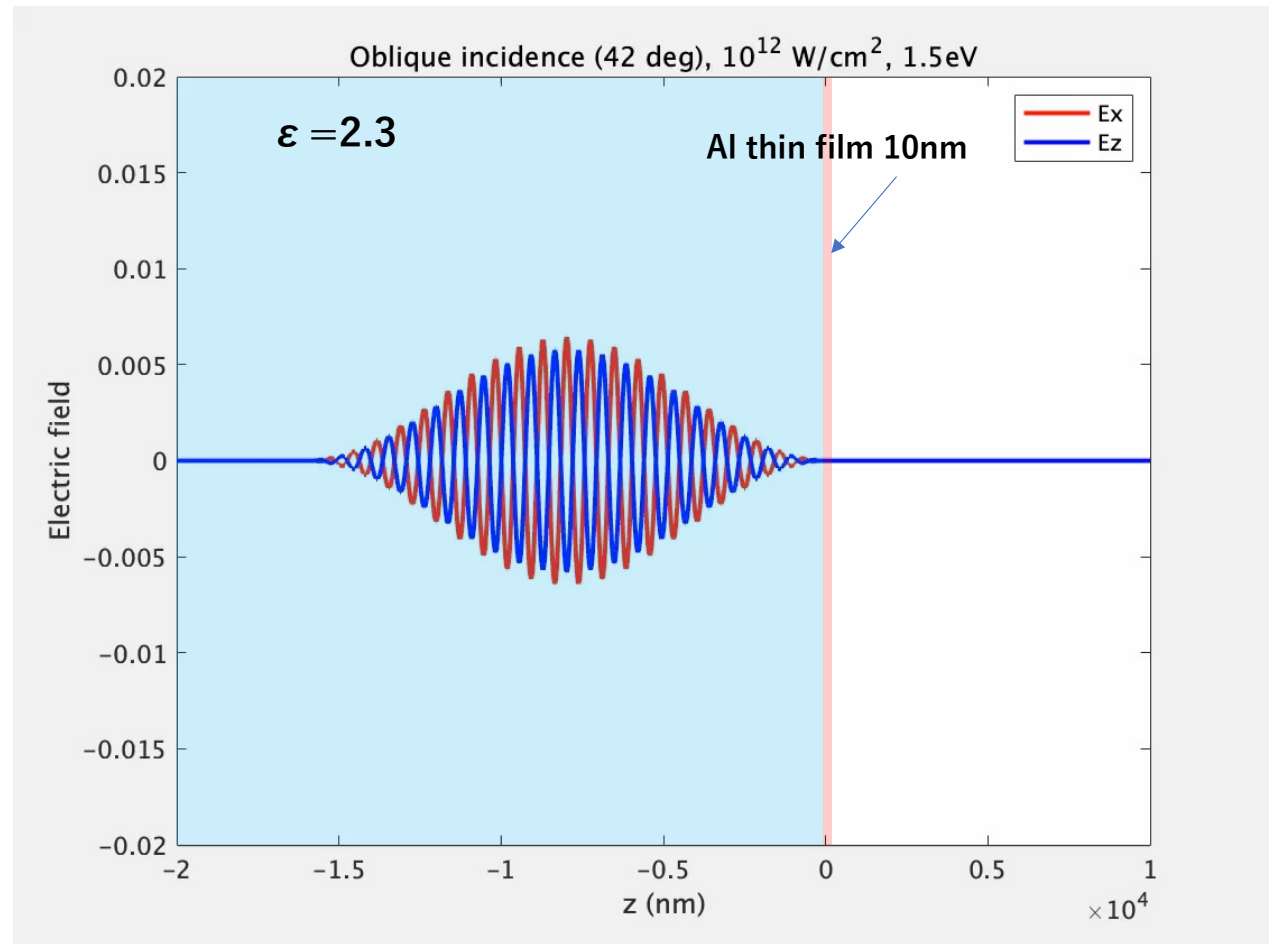
Multiscale Maxwell-TDDFT calculation at oblique incidence

Pulse information: $I=10^{12}$ W/cm², $hw=1.5$ eV, 42 deg., p -polarization

Kretschmann geometry



Surface plasmon mode appears when evanescent field appears in the vacuum region.



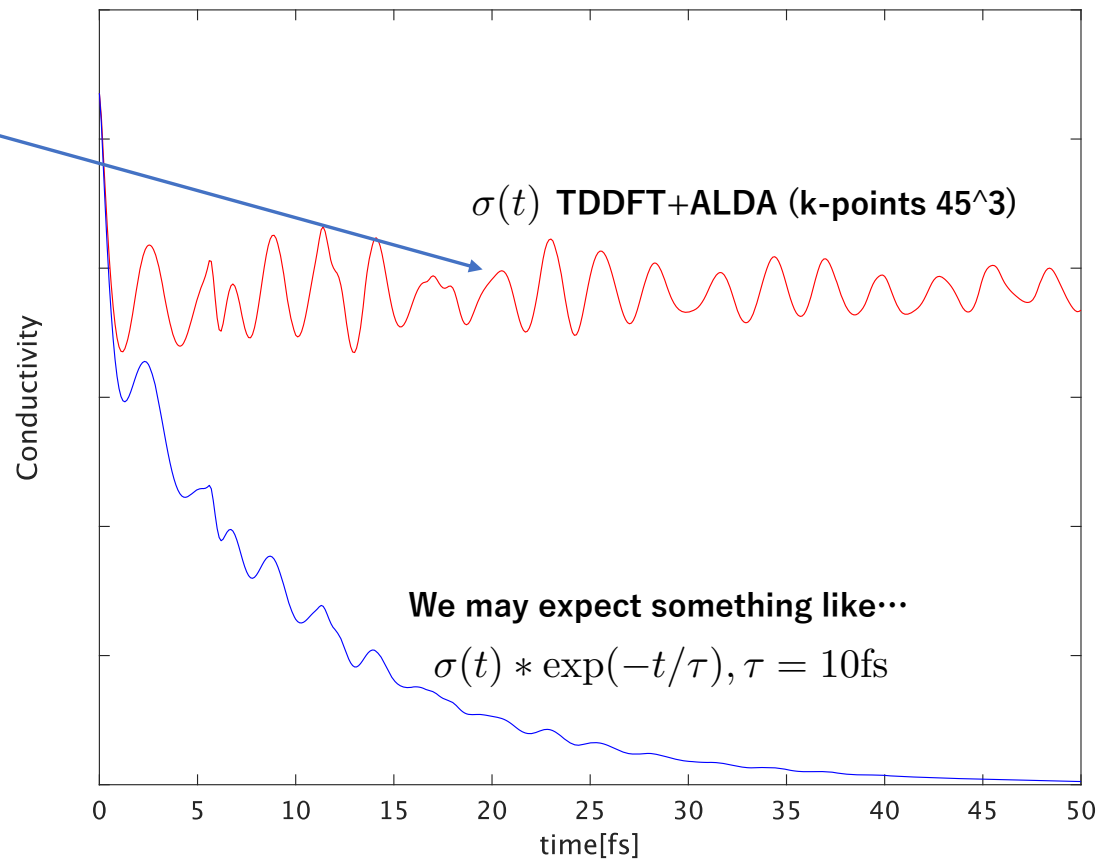
Contents

- About “Extreme Optics”
- Maxwell-TDDFT
- Some applications
- Maxwell-TDDFT at oblique incidence (under progress)
- **Dephasing and density-matrix unfolding (under progress)**

How reliable is TDDFT for metals?

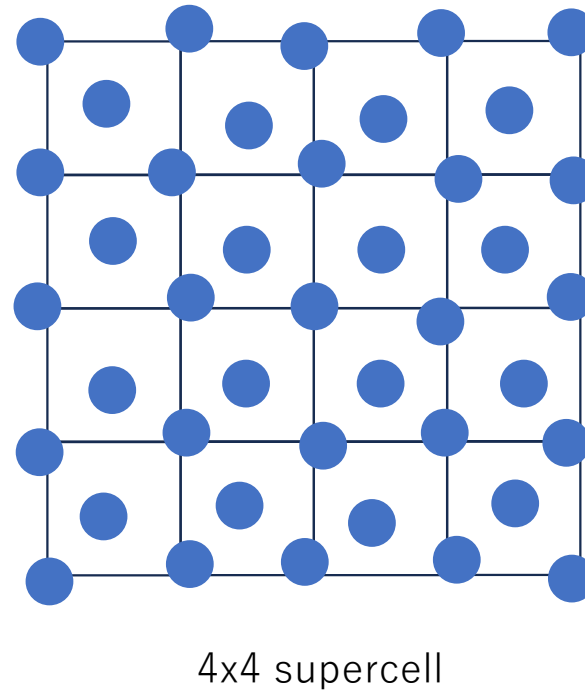
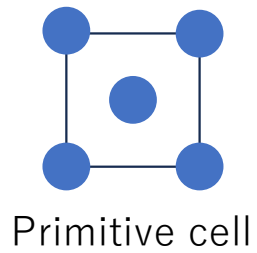
Linear conductivity of Aluminum (current after kick)

TDDFT+ALDA lacks Drude damping

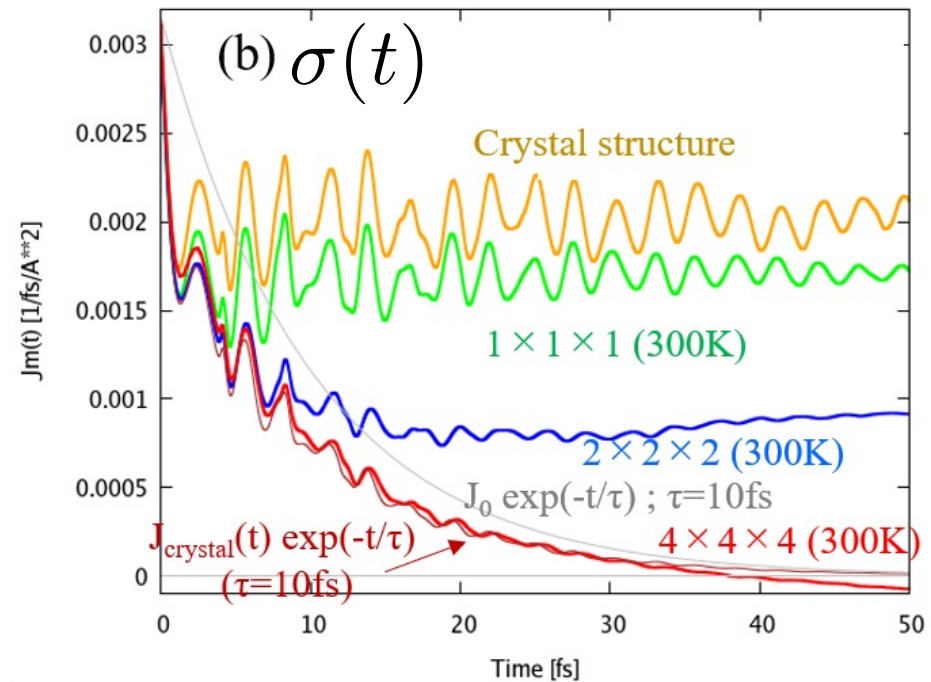
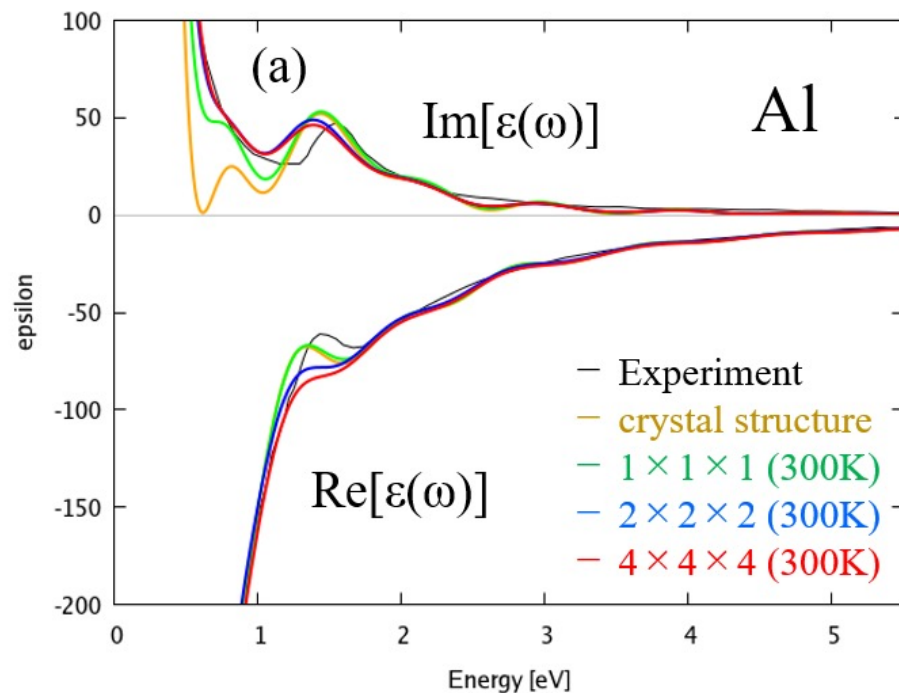


Simple method to incorporate electron-phonon scattering

Supercell calculation with thermally distorted (frozen) ionic positions



TDDFT for conductivity of Al: supercell calculations with thermally distorted (frozen) ionic positions



4x4x4 supercell containing 256 atoms is sufficient to describe Drude damping

Dephasing in crystalline solids

- Supercell calculation with thermal distortion (frozen atomic position) explains Drude damping of 10 fs time scale.
- Single configuration is enough to describe damping (ensemble average not necessary).

Next question:

Is description of dephasing using T_2 term supported microscopically?

$$\left[i \frac{\partial}{\partial t} + \frac{i(1 - \delta_{nn'})}{T_2} - \epsilon_{nn'\mathbf{k}} \right] \rho_{nn'\mathbf{k}}(t) \\ = \mathbf{E}(t) \sum_m (\rho_{nm\mathbf{k}}(t) d_{mn'\mathbf{k}} - d_{nm\mathbf{k}} \rho_{mn'\mathbf{k}}(t))$$

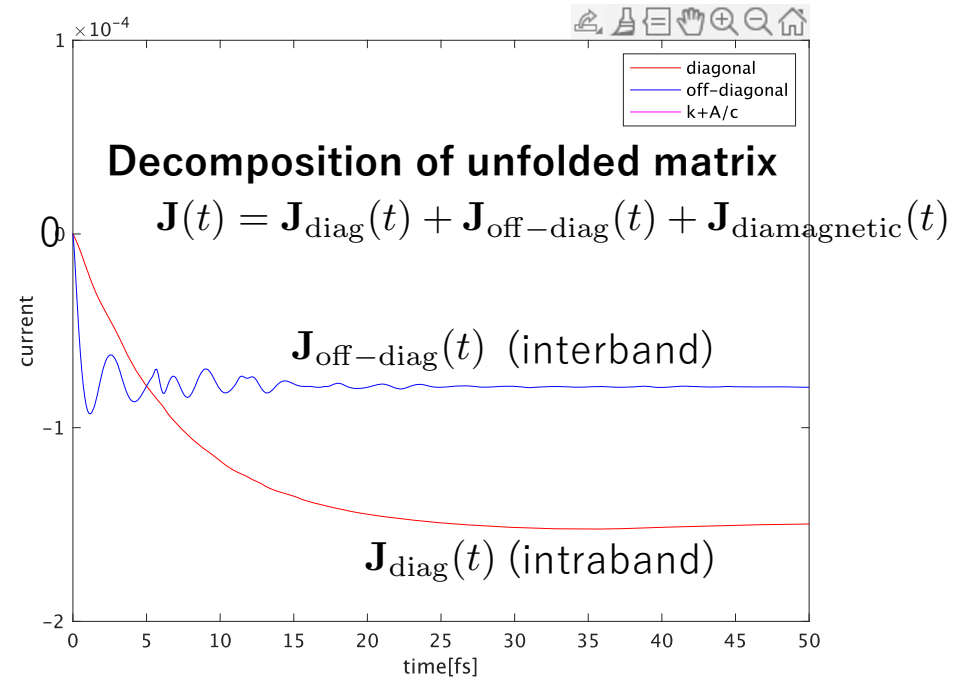
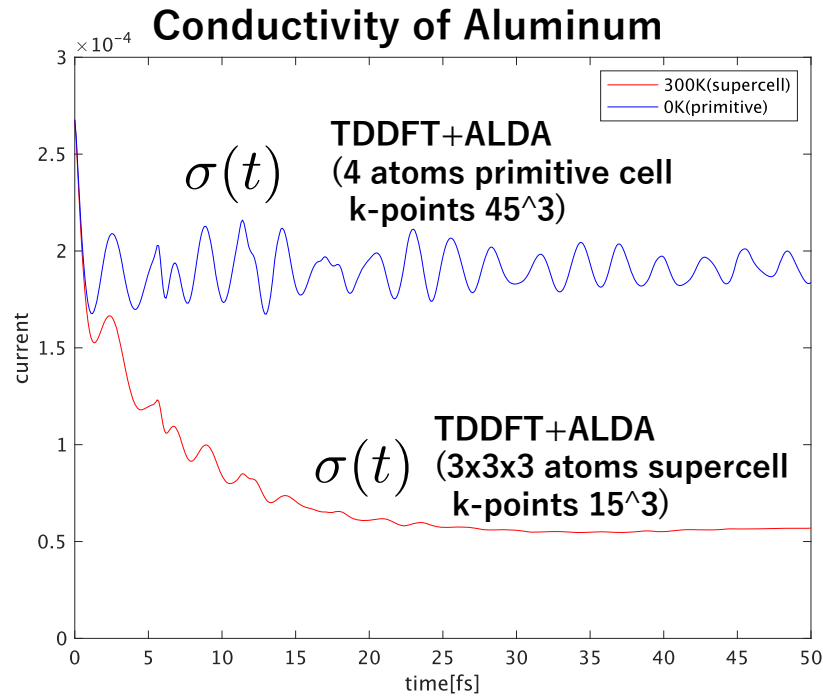
- Using density matrix, dephasing is often described as the attenuation of off-diagonal elements.
- Single-configuration supercell calculation is a pure state dynamics in folded k-space.
- Unfolding the density matrix into primitive-cell k-space, how damping looks like ?

In unfolded density matrix, how Drude damping looks like?

A. Yamada, K. Yabana, in preparation

Density-matrix unfolding $\rho_{mm'\mathbf{K}}(t)$ (supercell) \rightarrow $\rho_{nn'\mathbf{k}}(t)$ (primitive cell)

$$\mathbf{J}(t) = \frac{1}{V} \sum_{nn'\mathbf{k}} \rho_{nn'\mathbf{k}}(t) \langle u_{n\mathbf{k}} | (\mathbf{p} + \mathbf{k} + \mathbf{A}(t)/c) | u_{n'\mathbf{k}} \rangle$$



Drude damping appears in diagonal elements of primitive-cell density matrix

Summary

In current frontier of optics characterized by ultrafast, nonlinear, and nonlocal, traditional EM or QM approaches are not sufficient.

We develop first-principles electromagnetic analysis, combining EM and QM (Real-time TDDFT)

There are two connection methods: macroscopic (multiscale) and microscopic (single-scale)

Recent topics under progress includes oblique-incident Maxwell-TDDFT, dephasing description

Acknowledgement

Collaborators (SALMON project)



Atsushi Yamada
National Defence Academy Jpn.



Shunsuke Yamada
Kansai Photon Sci. Inst



Takashi Takeuchi
RIKEN



Arqum Hashmi
U. Tokyo



Mitsuharu Uemoto
Kobe Univ.



Yuta Hirokawa
Private Company



Shunsuke Sato
U. Tsukuba



Tomohito Otobe
Kansai Photon Sci. Inst.

Financial supports



Q-LEAP

Supercomputers

